Cyclohexane and Benzene Confined in MCM-41 and SBA-15: Confinement Effects on Freezing and Melting

Gilberte Dosseh,*,† Yongde Xia,§ and Christiane Alba-Simionesco

Laboratoire de Chimie physique, UMR CNRS 8000, Université de Paris Sud, Bâtiment 349, 91405 Orsay Cedex, France

Received: January 1, 2003; In Final Form: April 17, 2003

Using DSC scans and NMR line-shape analysis we have investigated the thermal properties of orientationally disordered crystal forming cyclohexane and benzene confined in highly ordered mesoporous materials MCM-41 and SBA-15. Phase transition temperatures and nature of the phases as a function of temperature were determined. In pores with diameters corresponding roughly to 10−30 molecular sizes ($4.7 \leq d \leq 14.0$ nm), important depressions of the melting point were observed and the confined material crystallizes only partially. The progressive melting of confined crystals detected by NMR is comparable to premelting effects usually observed in bulk molecular crystals. Here the surface of the pores plays the same role as the extended defects at the origin of premelting effects in bulk crystals. Unless in bulk crystals where premelting begins only a few degrees below the melting point, these effects spread out over a very large temperature range in confined crystals. The systematic analysis of various topology and surface interaction clearly showed that, besides the pore size, the other driving parameters for the phase transitions are the interactions between the confined fluids and the pore surface and the commensurability between the crystal symmetry and the surface structure. The melting point depression is larger in cyclohexane than in benzene due to the interaction between the π electrons of the benzene ring and the OH at the pore surface. In cyclohexane, the depression of the monoclinic to cubic transition temperature is always smaller than the melting point depression, inducing a decrease of the cubic phase temperature range with decreasing pore diameter. In 4.7 nm or narrower pores, both transitions disappear and liquid cyclohexane undergoes a glass transition even at cooling rate as small as 1 K/min. Benzene does crystallize in 4.7 nm pores but vitrifies in narrower pores. A phase diagram, presenting solid−solid-phase transition, melting and glass transition temperatures as a function of pore diameter was derived from experimental results.

Introduction

Thermal properties of confined phases have been widely studied but the interpretation of the results are complicated because of the addition of multiple effects such as geometry, size, surface properties and connectivity of the pores. Moreover, there appears to be a certain amount of disagreement in the interpretation of the results. The common model used for the interpretation of the results is the so-called Gibbs−Thomson equation.[1,2] According to this model, the difference between the normal and the confined melting points ΔT_m is proportional to the reverse diameter of the crystal formed within the filled pores. The sign of ΔT_m depends on the interaction between the pore wall and the confined material via the difference between the liquid−wall and the crystal−wall surface tensions ($\gamma_{lw} - \gamma_{cw}$). The Gibbs−Thomson equation, which is based on classical thermodynamics, does not hold for the narrowest pores due to surface heterogeneity (roughness and curvature) and finite size effects. Below a critical size, which depends on the confined fluid properties, freezing does not occur at all.[3,4] However, the role played by the pore geometry (pore shape, pore size distribution and pores interconnectivity) of the confining material, which is not explicit in the Gibbs Thomson equation, seems crucial: simulation results showed that departures from bulk freezing and melting temperatures in cylindrical pores are always lower than in slit pores with the same walls properties.[5] Experimental freezing of tetrachloromethane was observed in activated carbon fibers down to pore widths of 0.75 nm (less than two molecular diameters), whereas cylinders of several molecular sizes are necessary to allow crystallization.[5−8]

Most of the experiments on freezing and melting of organic compounds confined in pores have been done in porous systems such as Vycors, controlled porous glasses (CPG), or porous silica.[1,2,9−12] These three-dimensional confining porous systems are characterized by large distributions of pore size and pore interconnectivity,[13] inducing a disorder that may alter the properties of interest and complicate the interpretation of the results. Though simple geometry porous media such as MCM-41 and SBA-15 seem appropriate to study surface and size effects on the thermal properties of the confined fluids. MCM-41 and SBA-15 are mesoporous silica-walled materials that exhibit a regularly ordered two-dimensional hexagonal pore arrangement and narrow pore size distributions. MCM-41 pores are not interconnected and only microporous interconnections are found in SBA-15 pores.[14,15] The surface of both materials contains hydroxyl groups, which may experience specific interactions with molecules susceptible to having hydrogen

† Also at Département de Chimie, Université de Cergy-Pontoise, Bâtiment Sciences de la matière, 5 mail Gay-Lussac, 95031 Neuville Sur Oise Cedex, France.

§ Present address: B11, School of chemistry, The University of Nottingham, University Park, Nottingham NG7 2RD, United Kingdom.

10.1021/jp034003k CCC: $25.00
Published on Web 06/10/2003

bonds. Modifications of the surface of these materials could be achieved by grafting of hydrophobic groups. So, specific surface interaction effects on the properties of the confined compounds may be studied.

We have undertaken systematic studies of thermal properties of simple molecular compounds such as benzene and cyclohexane confined in MCM-41 and SBA-15 with pore diameters from 2.4 to 14.0 nm. Freezing and melting of these compounds confined in other nanoporous materials with silica walls have been studied elsewhere.[1,16,17] Few investigations were also done on solid−solid transitions of cyclohexane.[16,18] However, most of the experiments were made in three-dimensional confining disordered materials such as porous silica or CPGs. Gjerdåker et al. studied the cyclohexane confined in MCM-41 but they focused on the dynamical properties.[19] Gedat et al. were interested in rotational motion in the solid state of benzene confined in SBA-15.[20] Dubochet et al. investigated benzene and other molecular compounds confined in microemulsions,[21] regarded as quasi-spherical droplets, and pointed out the first evidence of a glass transition in confined benzene. Our main goal here is to compare our results to similar experiments performed on liquids confined in these disordered porous materials to extract some features that may be strictly attributed to confinement and/or surface interaction effects.

Cyclohexane can be viewed as a "globular" molecule with a hard sphere diameter of about 6 Å. The phase diagram of the bulk materials is well-known.[22] It forms a low-temperature rigid monoclinic crystal, which develops an anisotropic molecular motion with increased temperature. The lattice parameters of the monoclinic phase are $a = 11.23$ Å, $b = 6.44$ Å, $c = 8.80$ Å, and $\beta = 108.83°$. On heating, a monoclinic to cubic transition occurs at 186 K. The high-temperature solid phase is a plastic face centered cubic phase with a lattice parameter of 8.61 Å at 195 K. In this plastic phase molecules undergo reorientation, self-diffusion and ring inversion motions.[23,24] The rates of these motions increase with temperature up to the melting point at 280 K.

Benzene is a planar hexagonal shaped molecule. An averaged molecular diameter of 5 Å can be determined from pair correlation function.[25−27] The crystalline phase has an orthorhombic symmetry with lattice parameters $a = 7.460$ Å, $b = 9.666$ Å, and $c = 7.034$ Å.[28,29] Two types of molecular motions exist in solid benzene above 120 K: reorientation about the C_6 axis of the molecule and pipe defect self-diffusion. However, self-diffusion motions have lower rates in crystalline benzene than in plastic cyclohexane, leading to a melting entropy much higher in benzene (4.2R) than in cyclohexane (1.1R), where R is the perfect gas constant.

Besides their molecular sizes, benzene and cyclohexane have similar freezing and melting properties: they both form high temperature orientationally disordered crystals and their melting temperatures in the bulk are close (278.5 K for benzene and 280.0 K for cyclohexane). However, the molecular shapes and motions in their liquid and solid phases are quite different.

We have combined DSC and NMR experiments to study phase changes in benzene and cyclohexane confined in MCM-41 and SBA-15. DSC is one of the most convenient methods when dealing with phase transitions such as melting and freezing. The transition temperatures and their breadths may be determined easily by this method. ^{1}H NMR line-shape analysis is the ideal complementary method for our study. NMR spectra depend on the structure and the dynamics of the studied systems. The line shapes and line widths reflect the rate of molecular motions. When the molecules experience self-diffusion motions that are fast compared to NMR experimental time scale, the line is Lorentzian whereas systems with restricted motions give rise to broad Gaussian signals. Spectra of systems containing molecules or functional groups with different molecular mobilities usually show a composite signal, allowing the detection of two-phase systems, providing that molecular mobilities are significantly different in the two phases. Therefore, NMR measurements would be expected to notice events that lead to changes in the interactions between magnetic nuclei such as crystallization, melting, or progressive thermal activation of molecular mobility and provide a suitable method for the determination of phase changes temperature and phase mixtures when the DSC scans present very broad signals as in the case of confined systems. Moreover, depending on the experimental conditions, NMR spectra may be quantitative, allowing a precise determination of the amount of molecules in each phase.

Experimental Methods

1. MCM Synthesis and Characterization. MCM-41 and SBA-15 samples were synthesized in our laboratory at room-temperature according to the procedures described in refs 30 and 31, respectively. The two mesoporous materials are in powder form and their structural properties strongly depend on synthesis conditions. We characterized the matrixes used in this work by transmission electron microscopy, nitrogen adsorption, and small angle neutron scattering measurements. Transmission electron microscopy showed regular arrangement of the mesopores in a honeycomb fashion. The crystallites were usually hexagonal shaped with mesopores parallel to the axis of the prism. The sides of the basal plane vary from 0.02 to 0.5 μm and the length of the crystallites from 0.5 to 1 μm. The mesopores are running parallel to each other and may be slightly curved with curvature radii much more important than the crystallite sizes. Structure factors from small angle neutron scattering exhibit Bragg peaks reflecting the hexagonal structure of the pores. Nitrogen adsorption experiments (BET analysis) were used to determine pore diameters and pore volumes. In the case of MCM-41 materials we used a combination of both methods to determine pore diameters according to the procedure proposed by Kruk et al.[32] The detailed experimental procedures used for the synthesis and the characterization of the MCM-41 and SBA-15 samples were described elsewhere.[33,34]

2. Samples Preparation. The liquids were distilled at reduced pressure before sample preparations.

The bulk samples were sealed under vacuum in the NMR tube to avoid contamination with oxygen and water. To desorb water from the MCM-41 and SBA-15 pores, the empty matrixes were dried at 150 °C under vacuum for at least 24 h. The calculated volume of liquid was then injected into the empty pores with a syringe at room temperature. After an equilibration time of few hours, the samples were transferred in NMR tubes or DSC scans and sealed to avoid the sample contamination by oxygen and water.

3. DSC Measurements. The DSC measurements were performed using a Perkin-Elmer DSC2. A homemade temperature accessory was adapted to allow low-temperature measurements (down to 80 K). The temperature calibration was made with the bulk compounds. All the samples were slightly overloaded to detect the bulk and confined transition temperatures and a precise determination of the temperature depression. All the scans were carried out at heating or cooling rates of 10 $K \cdot min^{-1}$.

4. NMR Measurements. The ^{1}H NMR measurements were carried out at 250.13 MHz on a Bruker DPX 250 spectrometer

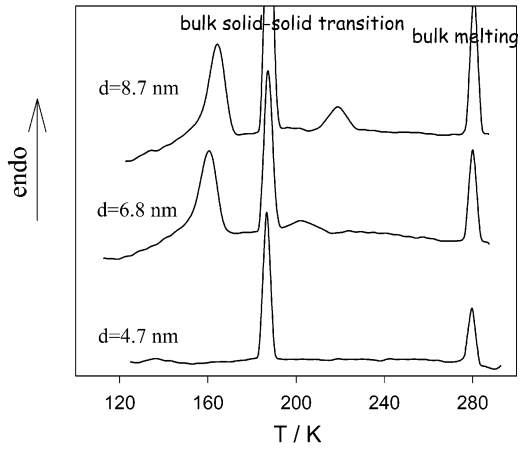

Figure 1. DSC scans of cyclohexane confined in SBA-15 with different pore diameters. Monoclinic to cubic and melting temperatures of the confined and the bulk crystals are shown.

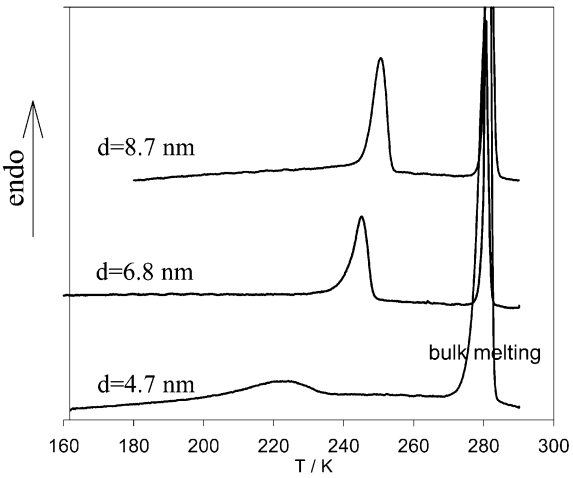

Figure 2. DSC scans of benzene confined in SBA-15 with different pore diameters showing melting temperatures of the confined and the bulk crystals.

equipped with a Bruker variable temperature controller. The temperature stability is ±1°. The temperature measurement at the sample was calibrated using methanol. All the experiments were done on heating at 2 K·min^{-1} with an equilibration delay of 10 min at each temperature before measurement. The free induction decays were recorded with a recycle time $>5T_1$.

Results

1. DSC Measurements. Figures 1 and 2 depict respectively DSC scans of the cyclohexane and benzene confined in SBA-15. All the scans present the melting points of the confined material and the bulk excess outside the pores. For both compounds, melting temperatures (and consequently crystallization temperatures) are lower than in their bulk form. The narrower the pore the more depressed is the transition temperature. In cyclohexane, the monoclinic to cubic transition temperature is also depressed. However, for each pore diameter, the extent of the depression of the solid−solid transition temperature is smaller than the extent of the melting temperature. The DSC signals due to the confined compounds are broad and have tails at their low-temperature sides. The narrower is the pore, the larger is the width of the peak and the longer is the tail. No thermal event corresponding to the confined liquid was detected for cyclohexane confined in pores equal to or smaller than 4.7 nm. Benzene crystallizes in the latter pores but does not in MCM-41. All the results shown in Figures 1 and 2 are in SBA-15 matrixes because both liquids do not crystallize in MCM-41. In bulk samples, phase transition temperatures are given by the onset of the transition peak on DSC scans. The same method cannot be used when dealing with confined phases because of the broadening of the transition peak. The transition temperatures were then commonly taken at the maximum of the peak.

Tables 2 and 3 summarize the DSC results on benzene and cyclohexane confined in silica-walled porous materials with different geometry and surface properties.

2. NMR Measurements. Figure 3 depicts the bulk spectra of benzene and cyclohexane as a function of temperature. The line shape of crystalline benzene does not change as a function of temperature, whereas the line width of cyclohexane decreases continuously with increased temperature in the cubic phase due to molecular motions: in the cubic phase, cyclohexane molecules acquire rapid rotational and self-diffusion motions, which induce a decrease of the line width, as shown in Figures 3 and 4. However, in both cases, close the melting point, the line becomes composite with a narrower line superimposed on a broader line, suggesting a two distinct molecular mobility system

TABLE 1: Structural Parameters of Mesoporous Silicates MCM-41 and SBA-15

samples	surf area (m^2/g)	pore vol (cm^3/g)	pore diam (nm)
MCM-41-C10	960	0.43	2.4
MCM-41-C14	947	0.52	3.1
MCM-41-C16	724	0.57	3.5
SBA-15A	560	0.67	4.7
SBA-15B	770	1.21	6.8
SBA-15C	690	1.34	8.7
SBA-15D	440	1.63	14.0

TABLE 2: Melting and Freezing Properties of Benzene[a]

samples	pore diam (nm)	ΔT_m (K)	fwhm (K)
bulk	∞	0	1.2
SBA-15A	4.7	59.3	30.0
SBA-15B	6.8	36.2	5.2
SBA-15C	8.7	31.0	4.8
SBA-15D	14.0	16.3	6.1
CPG[1]	4.0	37.3	22.0
CPG[1]	8.5	8.5	3.2
CPG[1]	15.6	3.6	2.0
microemulsion[21]	12.0	6.0	4.5

[a] ΔT_m represents the difference between the melting temperatures of the bulk and the confined crystals ($T_{m(bulk)} = 278$ K). fwhm represents the full width at half-maximum of the melting peak. The accuracy of the temperatures in our DSC measurements is ±0.7 K.

TABLE 3: Phase Transition Properties of Cyclohexane[a]

samples	pore diam (nm)	ΔT_{ss} (K)	fwhm (K)	ΔT_m (K)	fwhm (K)
bulk	∞	0	1.5	0	1.4
bulk[9]	∞	0	2	0	2
SBA-15D	14.0	12.1	8.1	25	14.0
SBA-15C	8.7	23.6	9.4	62	8.1
SBA-15B	6.8	27	10.0	73.0	13.0
porous silica[9]	4	12	12	29	22
porous silica[9]	7.5	8	6	15	3.2
porous silica[9]	15	3	6	12	2.0

[a] ΔT_{ss} is the difference between the monoclinic to cubic transition temperatures between the bulk and the confined crystals ($T_{ss(bulk)} = 186$ K). ΔT_m represents the difference between the melting temperatures of the bulk and the confined crystals ($T_{m(bulk)} = 278$ K). fwhm represents the full width at half-maximum of the peaks.

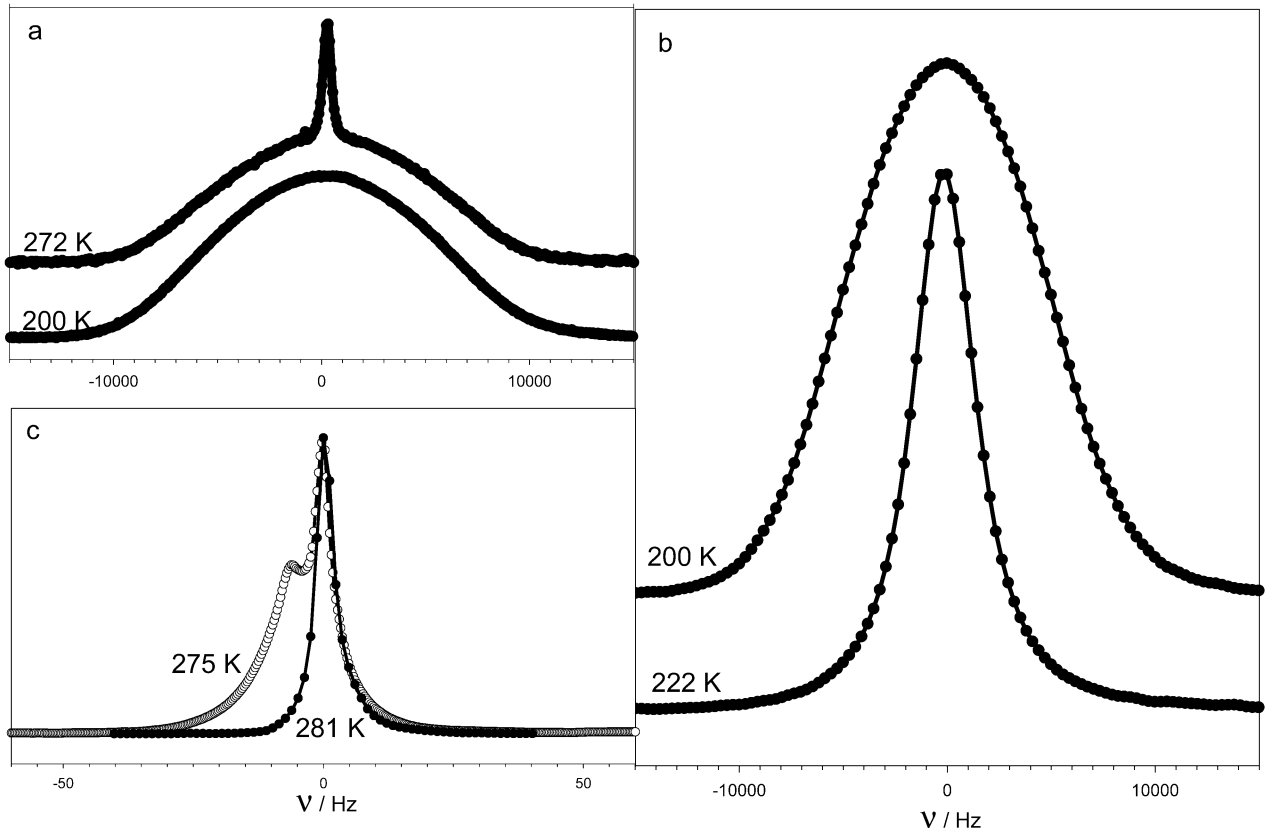

Figure 3. ^{1}H NMR spectra of bulk benzene and cyclohexane. (a) Melting of bulk benzene with an unchanged line width of the crystal. Additional premelting effects appear at 272 K. $T_m = 278$ K. (b) Cubic cyclohexane: the line width decreases when T increases ($T_{ss} = 186$ K and $T_m = 280$ K). (c) Premelting effects in cubic cyclohexane at 275 K.

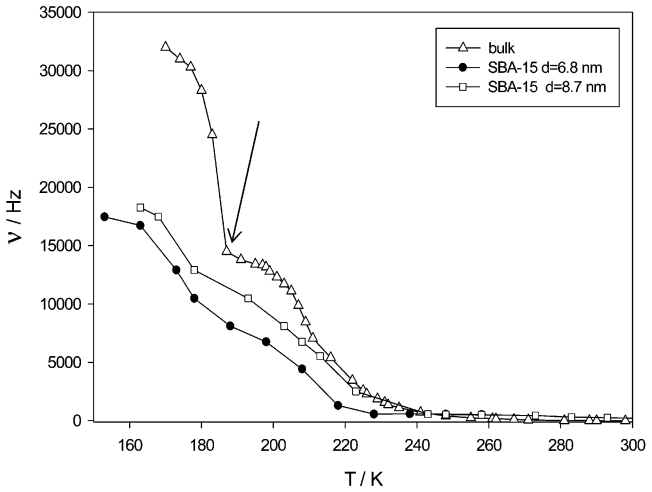

Figure 4. Line width of confined and bulk crystalline cyclohexane. The arrow locates the monoclinic to cubic transition.

(Figure 3a,c). Composite lines are usually observed in molecular crystals a few degrees below the melting point and are attributed to premelting effects.[23,35] The narrower line is due to liquidlike molecules, located at the grain boundaries, which experience higher frequency motions. The amount of molecules that contribute to the narrow line increases with increasing temperature and reaches 100% at a temperature that is considered as the melting temperature of the sample (Figure 5). Premelting has been interpreted as an interface initiated process, which is enhanced by the presence of impurities nonsoluble in the solid phase. The melting point of the sample decreases as the amount of impurities in the sample increases.

The monoclinic to cubic transition of cyclohexane in its bulk form is characterized by a sharp decrease in the line width, as depicted in Figure 4 (see the arrow). As melting, this transition presents pretransition phenomenon with the apparition of a small amount of cubic phase a few degrees below the calorimetric transition temperature. The NMR line is composite with a broad line (32 000 Hz) corresponding to the molecules in the monoclinic phase superimposed with a narrower line (13 000 Hz) due to the molecules in the cubic phase. The contribution of the narrower line increases with the temperature up to the solid−solid transition point. In the confined compounds that crystallized, the lines have two components in the whole studied temperature range, from 150 K to their melting point, suggesting two different molecular mobilities in the sample. On one hand, the broad solidlike line may be attributed to molecules of crystalline cyclohexane localized in the center of the pores as shown in Figure 6. On the other hand, a fraction of molecules, presumably those at the surface of the pores, are more mobile than those in the center of the pores and give rise to a Lorentzian liquidlike line. The widths of the two components decrease with increased temperature, suggesting an increase of the molecular mobilities of the two classes of molecules. On heating, the amount of liquidlike molecules increases with the temperature up to the melting points (Figure 5). Similar spectra were obtained for benzene in SBA-15 in agreement with Gedat et al. observations. They showed that in a 8.0 nm pore the liquidlike line persists down to 121 K. The same qualitative behavior was observed in bulk samples in a much narrower temperature range.

The transition points of the bulk materials detected by NMR and DSC are very close, whereas the confined systems always exhibit large transition temperature differences due to the broadening of the transitions. Unlike DSC, NMR may detect

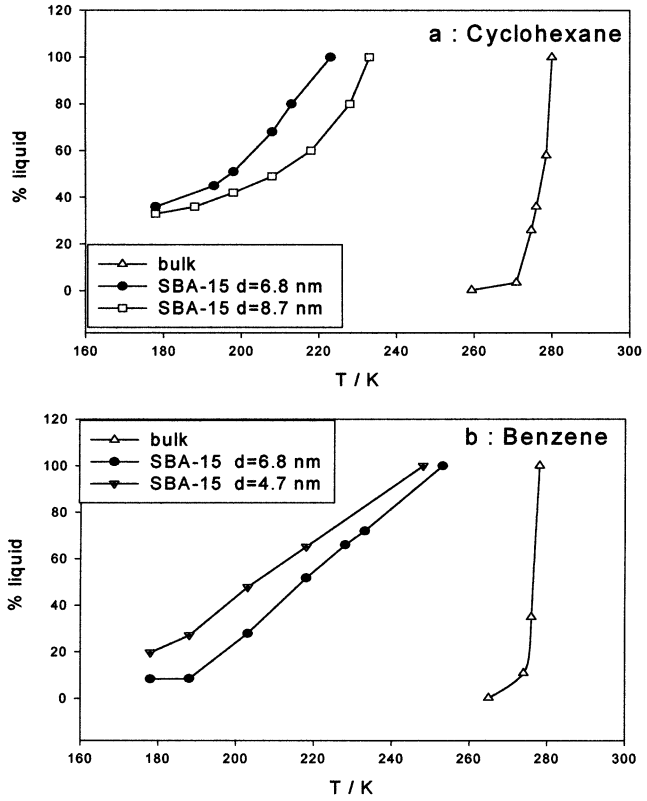

Figure 5. Liquid contribution to the spectra due to progressive melting as a function of temperature: (a) cyclohexane; (b) benzene. The relative errors in the measurements of the proportions of both phases is 5%.

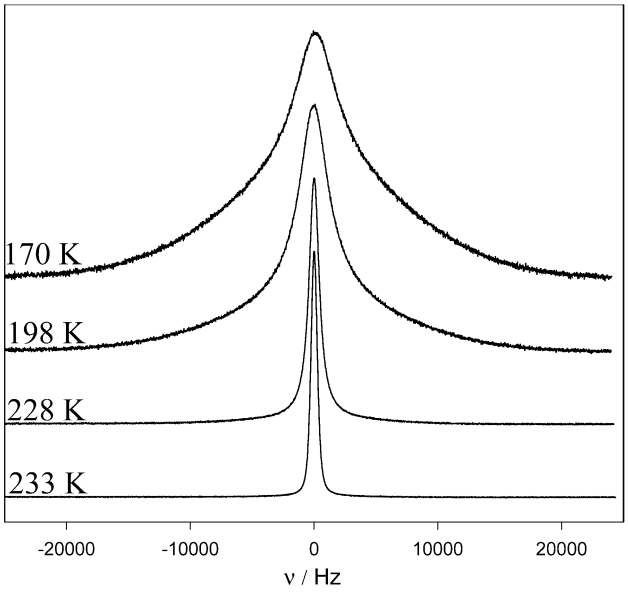

Figure 6. Melting of cubic cyclohexane confined in SBA-15 by ^{1}H NMR (d = 6.8 nm).

all the phases in the samples and the transition temperatures determined by NMR correspond to the total disappearance of a phase. Therefore, the melting point determined by proton NMR line-shape analysis are always higher than that determined by DSC in the confined samples.

In the smallest pores ($d \leq 3.5$ nm for benzene and $d \leq 4.7$ nm for cyclohexane), no crystallization occurs. On cooling, the NMR line remains Lorentzian down to very low temperatures ($T \leq 180$ K) for both liquids. Below this temperature, the line

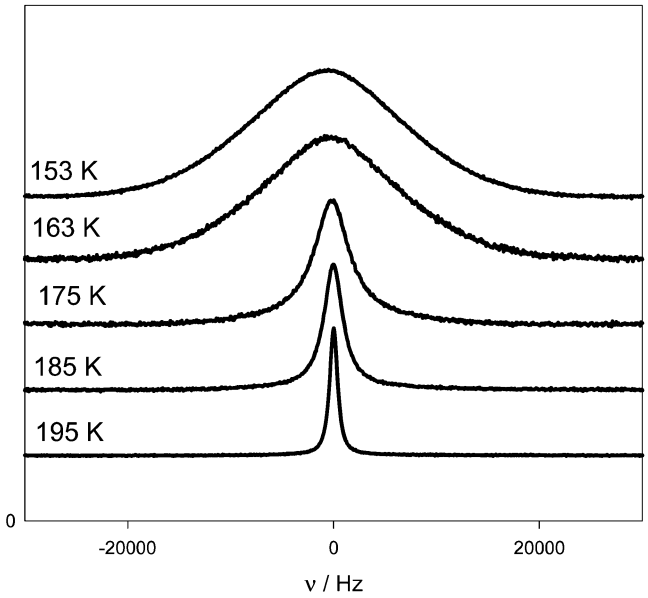

Figure 7. Viscous slowing down of the cyclohexane in MCM-41 (d = 3.5 nm) when approaching the glass transition in confined cyclohexane.

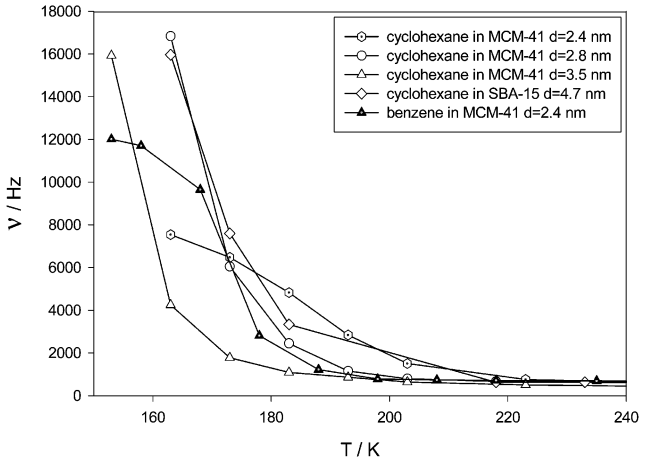

Figure 8. NMR line widths of cyclohexane confined in small pores (d < 6.8 nm). No crystallization occurs. The changes in the line width are due to the glass transition. Similar behavior is observed in confined benzene (d = 2.4 nm).

width increases sharply, forming a one-component broad Gaussian line (see Figure 7 for cyclohexane). On heating, the NMR line has only one component in the whole temperature range studied. No additional liquidlike line appears but the line width decreases suddenly between 153 and 175 K depending of the pore diameter (Figure 8). This behavior suggests a glass to liquid transition. The main thermodynamic feature characterizing a glass transition in calorimetry is a specific heat jump on heating. However, no signatures of glass transition or of crystallization were observed in the DSC scans due to the very small amount of materials inside the pores, which results in a thermal signal that is below the sensitivity limits of the instrument. More sensitive methods such as neutron scattering or adiabatic calorimetry are currently used to study the glass transition of benzene and detailed investigations on glass transition of confined benzene will be published elsewhere.[36]

Discussion

1. Crystallization and Melting. Concerning the crystallization and melting transitions, several points are discussed.

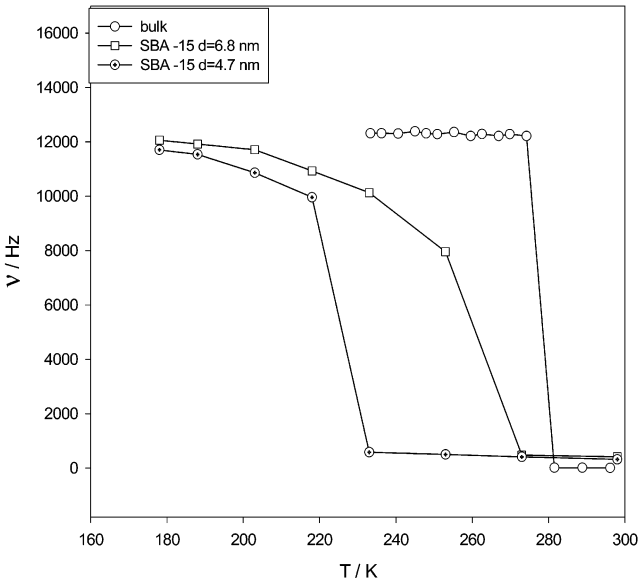

Figure 9. Line width of crystalline benzene as a function of temperature: the bulk benzene and benzene confined in SBA-15 (d = 4.7 and 6.8 nm).

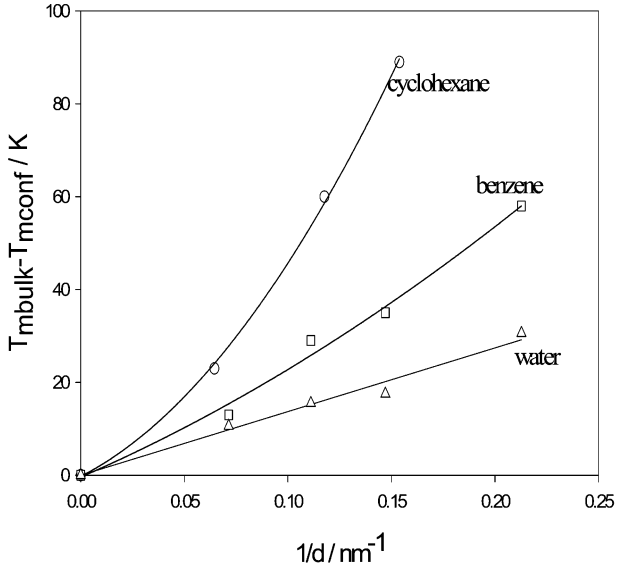

Figure 10. Cyclohexane (○), benzene (□), and water (△) confined in SBA-15: temperature depression as a function of the reverse pore diameter.

Quantitative results are summarized in Tables 2 and 3 and in Figure 9. The temperature depressions compared to the bulk are plotted as a function of the reverse pore diameter in Figure 10.

The first point concerns the broadening of the transition. Whatever the confining media, solid−solid transition of cyclohexane and melting of both compounds are characterized by a broad DSC peak (Figures 1 and 2). The narrower the pore, the larger the breath of the transition. This behavior is consistent with the evolution of the NMR signals in which the amount of liquidlike molecules increases with temperature up to the melting point (Figure 4). The DSC peak of benzene confined in a 4.7 nm pore has a breadth of 55 K and a full width at half-peak of 26 K. The broadening of the transition is usually at least partially attributed to pore size distribution. MCM-41 and SBA-15 are known to have narrower pore size distributions than interconnected mesoporous materials such as Vycors or CPGs. However, the breaths of the transitions or the full widths at half-peak maxima have comparable values in our experiments and in Mu and Malhotra or Jackson and McKenna experiments (Tables 2 and 3). Phase transitions in condensed matter are due to collective cooperative behavior of a macroscopically large number of atoms or molecules. A decrease of the system size or its dimensionality, when confined in mesopores, can strongly affect its behavior. In the pores where crystallization occurs, the NMR spectra clearly show partial crystallization of benzene and cyclohexane in the whole temperature range studied. Progressive layer-by-layer melting of the confined nanocrystals may rather cause this broadening, as illustrated by the ^{1}H NMR spectra. This behavior is comparable to the premelting effects in the bulk but is extended over a wider temperature range.

The second point focuses on the effect of geometrical confinement and wall interaction. Experimental studies on freezing and melting of confined organic compounds showed that crystallization is a quite complex process, as mentioned above. For very simple molecules with van der Waals type interactions, such as benzene or tetrachloromethane, the minimum pore size for crystallization is roughly 10 molecular sizes. Similar results were obtained by Monte Carlo simulation by Radhakrishan et al. where the molecules were modeled by one-site Lennard-Jones potentials.[8] For more complex molecules, crystallization depends also on the stability of the crystal and the ability to supercool in the bulk form. No crystallization was observed for fragile glass-forming liquids such as toluene or *o*-terphenyl confined in silica-walled porous materials with pore diameters larger than 15−20 molecular sizes.[1−3,34] For benzene or cyclohexane confined in cylindrical pores of roughly 10−20 molecular sizes, the fluids partially crystallize in a mixture of defective crystal and amorphous regions. In larger pores crystallization may be complete. Booth and Strange's results on cyclohexane confined in CPG showed that crystallization is completed below 250 K in pores of 20 nm and below 268 K in pores of 50 nm.[10] However, geometrical restriction is not the only cause of changes in thermal properties of confined fluids. Many factors such as molecular motions (including internal motions), crystal−wall interactions, crystal structure, and its commensurability with the wall structure may influence phase transition in confined fluids and the crystal stability. Because of its reduced size and its surface energy, a crystal growing inside a pore experiences compressive stress. On the basis of geometrical considerations, Warnock et al. suggested that the freezing temperature of a fluid confined in small pores is governed by a length scale r and the difference between the interfacial energies of the liquid and the solid with the wall.[37] The increase of the pressure inside the crystal, due to its curvature, leads to a change in melting temperature according to the Gibbs−Thomson equation:

$$T_{m(bulk)} - T_m(r_p) = \frac{2V_m T_{m(bulk)}(\gamma_{lw} - \gamma_{cw})}{r_p \Delta H_m}$$

where γ_{cw} and γ_{lw} are respectively the crystal−wall and liquid−wall interaction energy, $T_{m(bulk)}$ is the bulk melting point, r_p is the pore radius, V_m is the crystal molar volume, and ΔH_m is the molar melting enthalpy of the crystal. If $\gamma_{cw} < \gamma_{lw}$, the melting point of the confined crystal would be superior the bulk melting point. In such a situation, the crystal should nucleate at the pore walls and grow easily and the confined crystal would be more stable than the liquid above the bulk melting point. This behavior was experimentally observed in several molecular crystals confined in slit pores: benzene or carbon tetrachloride

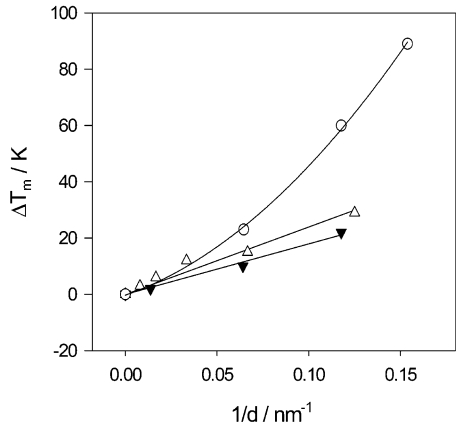

Figure 11. Dependence of temperature depression on surface properties for confined cyclohexane: present study (○), porous silica,[16] (△) and CPG[1] (▼).

confined in activated carbon fibers were reported to have an increase of their melting points.[38,39] Experiments on cyclohexane and octamethylcyclotetrasiloxane (OMCTS) confined in mica slit pores showed that cyclohexane and OMCTS froze respectively 17 and 6 K above the bulk melting point for a film thickness of about 7 molecular sizes.[40]

If $\gamma_{cw} > \gamma_{lw}$, the crystal should nucleate at the center of the pore inside the liquid. In such a situation, some liquid, near the wall may never crystallize and the melting point of the confined crystal is depressed. The smaller the pore the lower is the confined crystal melting point.

As cyclohexane and benzene are nonpolar molecules, $\gamma_{cw} > \gamma_{lw}$. They have a weak repulsive interaction with silica and a strong decrease of their freezing and melting points is observed when confined in silica-wall porous materials. Figure 10 shows the melting point depressions of cyclohexane, benzene, and water confined in SBA-15 as function of reverse pore diameter. For each pore size, confined cyclohexane has a larger melting point depression than benzene and water. Although silica-walled materials are considered hydrophobic, the interaction of the hydroxyl groups of the walls with water are stronger than with hydrocarbons such as benzene and cyclohexane, leading to a less depressed melting point. For comparison, experimental results on melting of cyclohexane in disordered silica-walled materials from Mu and Malhotra as well as Jackson and McKenna are presented in Figure 11. Unlike the MCM-41 and the SBA-15 we used, the surface properties of the porous materials used in their experiments were modified to increase their hydrophobicity. Jackson and McKenna grafted the surface of the CPG samples with trimethylsilyl groups. Mu and Malhotra dehydroxylated the porous silica surface under vacuum at 723 K. In both cases, the number of OH decreased, leading to an increase of the wetting of the surface by organic liquids. Figure 11 shows that the more hydrophobic is the pore surface, the smaller is the melting point depression and the less is the temperature depression. The difference in the behaviors of the three compounds cannot be attributed only to a difference in the ratio $(\gamma_{lw} - \gamma_{cw})/\Delta_m H$ because ΔT_m as a function of the reverse pore diameter is linear for water, almost linear for benzene, and not linear at all for cyclohexane. The fluid−wall interactions seem crucial in the melting point depression. These results are in agreement with different experiments that pointed out differences in the behavior of molecules at the surface and in the center of the pores. In a set of experiments on the dynamical behavior of confined fluids Jonas and co-worker studied dynamical behavior of confined fluids.[41−43] Their results as well as dielectric spectroscopy experiments performed by Kremer and co-workers[44−46] showed that surface interactions strongly affect the dynamics and consequently the phase changes in the confined fluids. Takei et al. studies on the evolution of the melting point temperature of *n*-hexane and benzene as a function of the number and the type of OH at the surface of silica-walled porous materials.[47] They showed that for a given pore size, an increase of the amount of OH results in a decrease of the melting temperature.

Figures 10 and 11 show that the agreement with the Gibbs−Thomson equation strongly depends on surface interaction in the pore diameter range used in our experiments: the fewer surface interactions with the confined molecules favorable, the more the departure from the Gibbs Thomson equation. Confined water, which has hydrogen bonds with the hydroxyl groups at the surface of the SBA pores, follows the Gibbs−Thomson relation whereas confined benzene and cyclohexane do not. Moreover, the departure from the Gibbs−Thomson relation is smaller for benzene, suggesting that the π electrons of benzene may interact with the hydroxyl groups.

NMR spectra show that in the SBA-15 pores, where cyclohexane and benzene do crystallize, a mixture of supercooled liquid and crystal is always observed well below the melting point. The amount of liquid increases in the whole temperature range studied. It is well-known that melting usually starts at the surface of the crystals, so it is not surprising to find a liquid layer at the interface. At this point, the question of the calculation of phase transition enthalpy in a confined system must be addressed. Calculation of phase change enthalpy requires the exact mass of the sample that undergoes the transition. As the confined fluids partially crystallize, it seems very difficult to determine the mass of fluid that really takes part in the phase transition in a calorimetry experiment. A part of the decrease of melting enthalpy of confined crystals reported in the literature is certainly due to this phenomenon. For a given pore size, the relative amount of liquid cyclohexane is larger than liquid benzene in the partially crystallized samples. The proportion of crystal phase involved in the measured melting enthalpy is smaller in cyclohexane than in benzene. This is another factor that may lead to a larger reduction of ΔT_m for cyclohexane.

2. Solid−Solid Transition of Cyclohexane. The cubic phase formation is always the first step required for the observation of the monoclinic phase. DSC scans for cyclohexane confined in SBA show that on cooling, when crystallization occurs, it is followed by the formation of the monoclinic phase. Once the cubic phase has been formed it should be easier to transform the crystal to the monoclinic phase at a lower temperature. On cooling or heating, the depression of the solid−solid transition is always smaller than the solid liquid transition point depression but no crossover nor triple point is achieved. Our results are in agreement with Mu and Malhotra or Shao and co-workers experiments, who used silica-walled interconnected pores in which the surfaces were modified to increase their hydrophobicity. Although the transition points are slightly lower in the case of our experiments in pores with nonmodified surfaces, the results show that surface interactions have less influence on the monoclinic to cubic transition than on the melting point (Figure 12), but a critical size of crystal or temperature range of crystal is required.

3. Glass Transition. In a deeply supercooled liquid, the correlation times of molecular motions increase continuously with decreased temperature. When the correlation times are large compared to the experimental time scale, the molecular motions

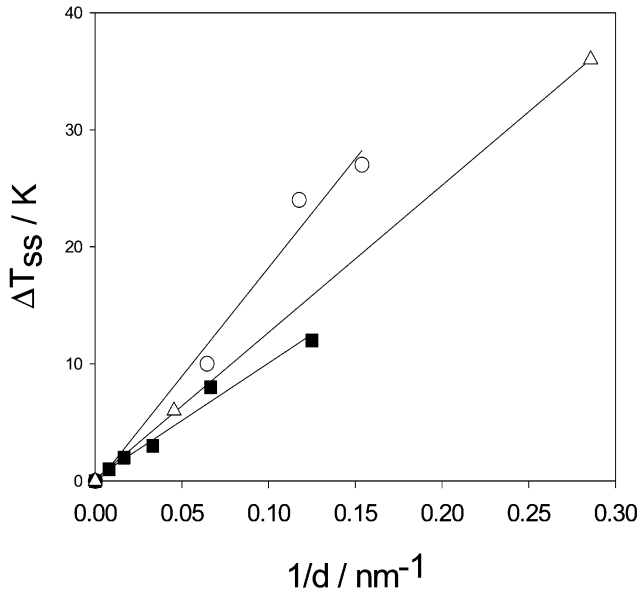

Figure 12. Monoclinic−cubic phase transition of confined cyclohexane in SBA-15: this work (○), porous silica,[16] (△) and ref 18 (■).

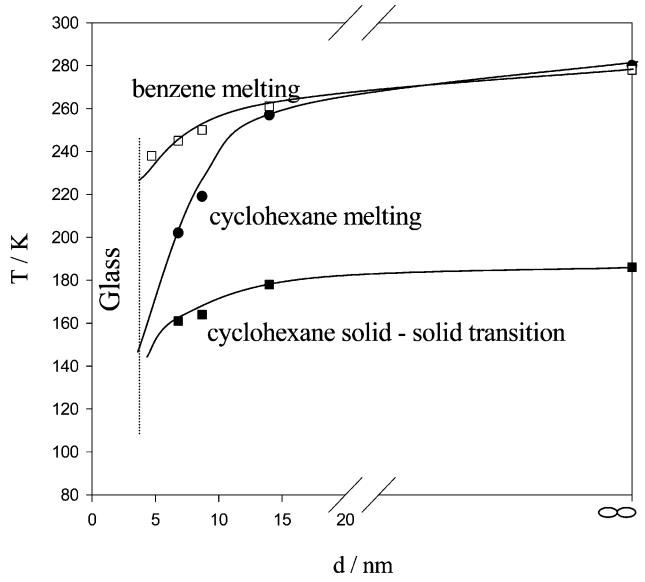

Figure 13. Phase diagram of benzene and cyclohexane in hexagonal ordered mesoporous silica materials (MCM-41 and SBA-15). The dashed line represents the minimum pore diameter for the crystallization to occur.

seem frozen. In the NMR experiment, the freezing of molecular motions leads to an increase of the line width. Unlike the line widths of the confined crystals, the confined glass line widths are not composite but a continuous change is observed. The "NMR glass transition" temperature is generally a few degrees higher than the calorimetric glass transition temperature because the NMR experiment time scale is smaller (tens of microseconds) than the calorimetric (1000 s in adiabatic calorimetry and 200 s in DSC) one.

Glass transitions were observed in confined benzene and cyclohexane, two compounds that usually do not undergo glass transitions in their bulk form at the cooling rates used for the confined materials in this work. The glass transition temperatures have a nontrivial evolution as a function of the pore diameter decrease, as observed for toluene[34] and benzene[36,48] by adiabatic calorimetry and neutron scattering. For benzene confined in 2.4 nm pores, a T_g of 175 K was determined by NMR (cf. Figure 8) in good agreement with adiabatic calorimetry and neutron scattering measurements (T_g = 170 K) by Xia et al.[48] quite higher than a "pseudo" bulk T_g of 121 K, estimated from microemulsion experiments.[21] Confined cyclohexane has a similar behavior for pore diameters between 2.4 and 4.7 nm. The whole transition is observed only for the smallest pore diameter: $T_g \sim 185$ K for $d = 2.4$ nm. For the other pore diameters, the glassy state is not completely reached (see Figure 8). A more detailed study on the effect of confinement and pore surface properties on glass transition in confined molecular liquid are published elsewhere.[34,36,48]

4. Phase Diagrams. On the basis of the above analysis, several phase transitions and temperature ranges of each phase can be summarized and plotted on a diagram.

As confinement induces different and sometimes very rich phase behavior, diagrams may be derived from confined systems studies. According to the interaction in interest, a different type of phase diagram may be drawn from confinement studies. We present here a diagram where the constraint induced by pressure is replaced by the geometric restriction induced by confinement.

Pore diameter versus temperature phase diagrams of confined cyclohexane and benzene are presented in Figure 13. The range of temperature of the crystalline phase decreases with pore diameter down to zero in pores smaller than 4.7 nm, which corresponds roughly to 10 molecular diameters. Below this pore diameter, no crystallization and no solid−solid phase transition were observed. Nevertheless, unlike the bulk materials, a glass transition line may be drawn on the diagram for both confined compounds and a new domain due to the glass, which is absent in the bulk materials, appears on the phase diagram.

However, because of the variety of geometry and surface interactions in mesoporous materials, such a diagram may change with the geometry of the pores and surface interaction and is not unique.

Another kind of diagram, based on the adsorbed fluid−wall interaction, was proposed by Radhakrishnan et al. and applied to slit pores.[49] In their model, the main parameters are the pore width and a parameter α that measures the ratio of the fluid−wall and the fluid−fluid interaction. The value of α determines the direction of change in the freezing temperature and the presence of new phases, such as hexatic phases. Their phase diagram represents the ratio between the freezing temperatures of the confined fluids and the bulk fluid as a function of the α parameter. The advantages of their diagram are that all the molecules may be represented on the same diagram. However, such a diagram must be drawn for each pore size and each pore topology.

Conclusion

Freezing and melting studies on confined fluids showed that multiple parameters intervene for the confinement effects on phase transition. The influence of many parameters such as the surface interaction, the global dynamics of the liquid, and the nucleation rate on the phase transitions in the confined fluid are not yet clear. The relative parts of geometrical confinement and fluid−wall interaction are still difficult to separate. Besides these effects, the topology of the confining matrix may play a crucial role. To disentangle all these parameters, systematic studies with surface modifications with constant topology and pore size are in progress. The modification of the strength of the hydrogen bonds at the surface and the increase of the surface hydrophobicity by grafting organic function may be helpful for the modification of the confined fluid−wall surface tension at constant topology.

Acknowledgment. We are grateful to Dr. Denis Morineau and Prof. Keith Gubbins for helpful discussions.

References and Notes

(1) Jackson, C. L.; McKenna, G. B. *J. Chem. Phys*. **1990**, *93*, 9002.
(2) Jackson, C. L.; McKenna, G. B. *Chem. Mater*. **1996**, *8* (8), 2128.
(3) Dosseh, G.; Morineau, D.; Alba-Simionesco, C. *J. Phys. IV* **2000**, *10* (Pr7), 99.
(4) Morishige, K.; Kawano, K. *J. Chem Phys.* **2000**, *112*, 11023.
(5) Maddox, M.; Gubbins, K. E. *J. Chem Phys.* **1997**, *107*, 9659.
(6) Kaneko, K.; Watanabe, A.; Iiyama, T.; Radhakrishnan, R.; Gubbins, K. E. *J. Phys. Chem.* **1999**, *103*, 7061.
(7) Watanabe, A.; Kaneko, K. *Chem. Phys. Lett*. **1999**, *305*, 71.
(8) Sliwinska-Bartkowiak, M.; Radhakrishnan, R.; Gubbins, K. E. *J. Chem. Phys.* **2000**, *112*, 11048.
(9) Mu, R.; Xue, Y.; Henderson, D. O.; Frazier, D. O. *Phys. Rev. B* **1996**, *53*, 6041.
(10) Booth, H. F.; Strange, J. H. *Mol. Phys.* **1998**, *93*, 263.
(11) Strange, J. H.; Rahman, M.; Smith, E. G. *Phys Rev. Lett*. **1993**, *71*, 3589.
(12) Krim, J.; Coulomb, J. P.; Bouzidi, J. *Phys. Rev. Lett.* **1987**, *58*, 583.
(13) Levitz, P. *Adv. Colloid Interface Sci*. **1998**, *76*−*77*, 71.
(14) Impéror-Clerc, M.; Davidson, A. *J. Am. Chem. Soc*. **2000**, *122*, 11925.
(15) Ravikovitch, P. I.; Neimark, A. V. *J. Phys. Chem. B* **2001**, *105*, 6817.
(16) Mu, R.; Malhotra, V. M. *Phys. Rev. B* **1991**, *44* (9), 4296.
(17) Asknes, D. W.; Gjerdåker, L. *J. Mol. Struct.* **1999**, *475*, 27.
(18) Shao, Y.; Hoang, G.; Zerda, J. W. *J. Non-Cryst. Solids* **1995**, *182*, 309.
(19) Gedat, E.; Schreiber, A.; Albrecht, J.; Emmler, Th.; Shenderovich, I.; Findenegg, G. H.; Limbach, H.-H.; Buntkowsky, G. *J. Phys. Chem. B* **2002**, *106*, 1977.
(20) Gjerdåker, L.; Aksnes, D. W.; Sørland, G. H.; Stöcker, M. *Micropor. Mesopor. Mater.* **2001**, 42, 89.
(21) Dubochet, J.; Adrian, M.; Teixeira, J.; Alba, C. M.; Kadiyala, R. K.; MacFarlane, D. R.; Angell, C. A. *J. Phys. Chem.* **1984**, *88*, 6727.
(22) Kahn, R.; Fourme, R.; André, D.; Renaud, M. *Acta Crystallogr. B* **1973**, *29*, 131.
(23) Dosseh, G.; Fressigne, C.; Fuchs, A. H. *J. Phys. Chem. Solids* **1992**, *53*, 203.
(24) McGrath, K. J.; Weiss, R. G. *Langmuir* **1997**, *13*, 4474.
(25) Lowden, L. J.; Chandler, D. *J. Chem. Phys.* **2002**, *116*, 1147.
(26) Bartsch, E.; Bertagnolli, H.; Chieux, P. *Ber. Bunsen-Ges. Phys. Chem.* **1985**, *89*, 147.
(27) Morineau, D.; Alba-Simionesco, C. *J. Chem. Phys.* **2003**, *118*, 9389.
(28) Cox, E. G. *Rev. Mod. Phys.* **1958**, *30*, 159.
(29) Cox, E. G.; Cruickshank, D. W. J.; Smith, J. A. S. *Proc. R. Soc. London, Ser. A* **1958**, *247*, 1.
(30) Grün, M.; Lauer, I.; Unger, K. *Adv. Matter*. **1997**, *9*, 254.
(31) Zhao, D.; Feng, J.; Huo, Q.; Melosh, N.; Frederickson, G. H.; Chmelka, B. F.; Stucky, G. D. *Science* **1998**, *279*, 548.
(32) Kruk, M.; Jaroniec, M.; Sayan, A. *Chem. Mater*. **1999**, *11*, 492.
(33) Morineau, D.; Dosseh, G.; Alba-Simionesco, C.; Llewellyn, P. *Philos. Mag. B* **1999**, *11*−*12*, 1847.
(34) Morineau, D.; Xia, Y.; Alba-Simionesco, C. *J. Chem. Phys.* **2002**, *117*, 1753.
(35) Dosseh, G.; Fuchs, A. H. *Z. Naturforsch. A* **1991**, *46*, 917.
(36) Xia, Y.; Morineau, D.; Dosseh, G.; Alba-Simionesco, C. To be published.
(37) Warnock, J.; Awschalom, D. D.; Shafer, M. W. *Phys. Rev. B* **1986**, *57*, 1753.
(38) Kaneko, K.; Watanabe, A.; Iiyama, T.; Radhakrishnan, R.; Gubbins, K. E. *J. Phys. Chem.* **1999**, *103*, 7061.
(39) Watanabe, A.; Kaneko, K. *Chem. Phys. Lett*. **1999**, *305*, 71.
(40) Klein, J.; Kumacheva, E. *J. Chem. Phys.* **1998**, *108*, 6996.
(41) Koziol, P.; Nelson, S. D.; Jonas, J. *Chem. Phys. Lett*. **1993**, *201*, 383.
(42) Korb, J. P.; Malier, L.; Cros, F.; Shu, X.; Jonas, J. *Phys Rev. Lett*. **1996**, *77*, 2312.
(43) Korb, J. P.; Shu, X.; Cros, F.; Malier, L.; Jonas, J. *J. Chem. Phys.* **1997**, *107*, 4044.
(44) Cramer, C.; Cramer, T.; Arndt, M.; Kremer, F.; Naji, L.; Santannarius, R. *Mol. Cryst. Liq. Cryst.* **1997**, *303*, 1647.
(45) Cramer, C.; Cramer, T.; Arndt, M.; Kremer, F.; Naji, L.; Santannarius, R. *J. Chem. Phys.* **1997**, *106*, 3730.
(46) Huwe, A.; Arndt, M.; Kremer, F.; Haggenmuller, C.; Behrens, P. *J. Chem. Phys.* **1997**, *107*, 9699.
(47) Takei, T.; Konishi, T.; Fuji, M.; Watanabe, T.; Chikazawa, M. *Thermochim. Acta* **1995**, *267*, 159.
(48) Alba-Simionesco, C.; Dosseh, G.; Dumont, E.; Frick, B.; Geil, B.; Morineau, D.; Teboul, V.; Xia, Y. *EPJ Direct*, in press.
(49) Radhakrishnan, R.; Gubbins, K. E.; Sliwinska-Bartkowiak, M. *J. Chem. Phys.* **2002**, *116*, 1147.